2005 International Symposium on Nonlinear Theory and its Applications (NOLTA2005)
Bruges, Belgium, October 18-21, 2005

Signal Prediction Using Active Filters

Mantas Meškauskas, Arūnas Tamaševičius, Kęstutis Pyragas and Gytis Mykolaitis

Semiconductor Physics Institute
A. Goštauto 11, Vilnius LT-01108, Lithuania
Email: mantas.meskauskas@ff.vu.lt, tamasev@pfi.lt

Abstract–An extremely simple analogue circuit employing RC active filters is suggested for prediction of time-continuous signals on a real time scale. It includes operational amplifiers based units: an inverter, one or more integrators and an adder. The performance of the predictor is demonstrated experimentally using different types of waveforms, from periodic to chaotic signals.

1. Introduction

Various predictors are employed to estimate the future states of a system and are applied to many engineering devices: to speech signal processors, industrial process controllers, simulators of mechanical movements, etc. Commonly predictors are based on digital methods and need digital computing equipment. In some cases, e.g. prediction on a real time scale or fast control, digital techniques appear rather complicated and expensive. Alternatively analogue electronics [1] seems to be advantageous, for example to control fast chaos [2].

In this paper we describe a very simple and inexpensive electronic circuit based on RC active filters. It is convenient for short-term prediction, especially in the cases when the system model is not available.

2. Mathematical Background

Considering an arbitrary time-continuous signal $S(t)$ and requesting its predicted waveform to be $S(t+\tau)$, where τ is the prediction time, the predictor according to the 'shift in time' theorem of the Laplace transform should have an exponential transfer function [1]:

$$H(p) = \exp(\tau p). \tag{1}$$

Thus the electronic circuit should also have the transfer function given by Eq. (1). The design of the circuit is based on a set of one-way coupled RC filters described:

$$\begin{aligned} &\varepsilon \dot{x}_1 = -x_0 - x_1, \quad x_0 = -S(t), \\ &\quad ... = ..., \\ &\varepsilon \dot{x}_n = -x_{n-1} - x_n. \end{aligned} \tag{2}$$

Here ε is an integration parameter, $x_1,\ldots x_n$ are the dynamical variables. The output signal we present in the form of a linear combination:

$$S(t+\tau) = \sum_{i=0}^{n} a_i x_i(t). \tag{3}$$

Applying the Laplace transformation to Eq. (2) and Eq. (3) we obtain

$$\begin{aligned} &x_1(p) = -x_0(p)(\varepsilon p + 1)^{-1}, \quad x_0(p) = -S(p), \\ &\quad ... = ... \\ &x_n(p) = -x_{n-1}(p)(\varepsilon p + 1)^{-1}, \end{aligned} \tag{4}$$

$$S(+\tau, p) = \sum_{i=0}^{n} a_i x_i(p). \tag{5}$$

The weight coefficients a_0, a_1, ..., a_n in (5) are just the same as in (3) and should be determined separately for a specific order of a predictor.

2.1. First-Order Predictor (n = 1)

Taylor series expansion of $x_1(p)$ in (4) for small ε up to term εp yields

$$x_1(p) = -x_0(p)(1 - \varepsilon p). \tag{6}$$

Then by substituting (6) in (5) for $n = 1$ the first-order transfer function can be presented in the following form

$$H_1(p) = S(+\tau, p)/S(p) = -a_0 + a_1(1 - \varepsilon p). \tag{7}$$

On the other hand the transfer function (1) can be also expanded for small prediction times τ to power τp:

$$H_1(p) = 1 + \tau p. \tag{8}$$

From (7) and (8) we obtain

$$\begin{aligned} a_0 &= -(1 + \tau/\varepsilon), \\ a_1 &= -\tau/\varepsilon. \end{aligned} \tag{9}$$

Evidently, the ratio τ/ε can be chosen arbitrary, e.g. $\tau = 3\varepsilon$. In this case

$$a_0 = -4, \quad a_1 = -3.$$

2.2. Second-Order Predictor (n = 2)

For $n = 2$ Eqs. (4) read

$$\begin{aligned} x_1(p) &= -x_0(p)(\varepsilon p + 1)^{-1}, \\ x_2(p) &= -x_1(p)(\varepsilon p + 1)^{-1} = x_0(p)(\varepsilon p + 1)^{-2}. \end{aligned} \tag{10}$$

Taylor series expansion of $x_1(p)$ and $x_2(p)$ in (10) for small ε up to terms $\propto \varepsilon^2 p^2$ gives

$$\begin{aligned} x_1(p) &= -x_0(p)(1 - \varepsilon p + \varepsilon^2 p^2), \\ x_2(p) &= x_0(p)(1 - 2\varepsilon p + 3\varepsilon^2 p^2). \end{aligned} \tag{11}$$

By substituting (11) in (5) for $n = 2$ the second-order transfer function can be presented in the following form

$$H_2(p) = -a_0 + a_1(1 - \varepsilon p + \varepsilon^2 p^2) - \\ - a_2(1 - 2\varepsilon p + 3\varepsilon^2 p^2). \quad (12)$$

On the other hand the transfer function (1) can be also expanded for small prediction times τ to power $\tau^2 p^2$:

$$H_2(p) = 1 + \tau p + \tau^2 p^2 / 2. \quad (13)$$

From (12) and (13) we obtain the weight coefficients

$$a_0 = -(1 + 2\tau/\varepsilon + \tau^2/2\varepsilon^2), \\ a_1 = -(3\tau/\varepsilon + \tau^2/\varepsilon^2), \quad (14) \\ a_2 = -(\tau/\varepsilon + \tau^2/2\varepsilon^2).$$

It is convenient to set $\tau = \varepsilon$. Then the weight coefficients are

$$a_0 = -3.5, \quad a_1 = -4, \quad a_2 = -1.5.$$

3. Hardware Implementation

The electronic circuits characterized by the transfer functions, either $H_1(p)$ or $H_2(p)$ for the first- and the second-order predictors, respectively, are implemented using operational amplifiers (opamps) based units: invertors, inverting integrators, and inverting adders [3]. Firstly, to implement the equality $x_0 = -S(t)$ in (2) a simple invertor is required. Secondly, the differential equations in (2) can be easily solved by means of inverting integrators. Number of the integrators is just the order of the predictor n. Finally, the linear combination (3) can be conveniently implemented by means of a single inverting adder, since the weight coefficients a_0, a_1, and a_2 all are negative.

3.1. First-Order Predictor

Circuit diagram of the first-order predictor is shown in Fig. 1. It includes an inverter, an inverting integrator and an inverting adder.

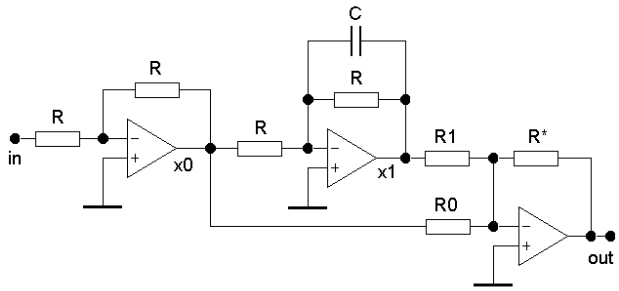

Fig. 1. First-order predictor. Opamps are the LM741.

The integration parameter is determined by the RC time constant, $\varepsilon = RC$. The feedback resistance in the adder $R^* = R$. The values of R_0 and R_1 are defined by the corresponding weight coefficients:

$$R_0 = R/|a_0|, \quad R_1 = R/|a_1|. \quad (15)$$

3.2. Second-Order Predictor

Circuit diagram of the second-order predictor is presented in Fig. 2. It includes an inverter, two inverting integrators and an inverting adder.

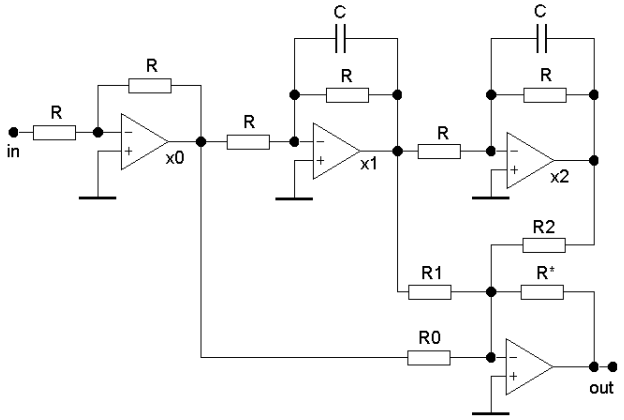

Fig. 2. Second-order predictor. Opamps are the LM741.

The integration parameter ε is the same as in the previous case. The values of R_0, R_1 and R_2 are defined by the corresponding weight coefficients:

$$R_0 = R/|a_0|, \quad R_1 = R/|a_1|, \quad R_2 = R/|a_2|. \quad (16)$$

Normally, the resistance R^* is set to be equal to R. However, if the coefficients a_i are large, e.g. when $\tau >> \varepsilon$, the input resistances R_0, R_1, R_2 can appear unacceptably small. Then they can be increased, say by a factor of 10, provided the R^* also is increased by the same factor to have the required gain of the adder.

3.3. Signal Generator

To test the performance of the predictors we used the signals generated by an electronic oscillator (Fig. 3) similar to one described in [4]. The main difference of the circuit presented in Fig. 3 compared to the oscillator in [4] is that we employed here analogue computer units, i.e. three inverting integrators and an invertor instead of a noninverting amplifier and the 3rd order L–C–C resonator.

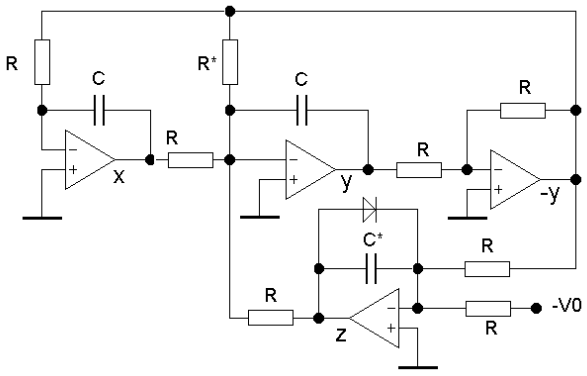

Fig. 3. Signal generator. Opamps are the LM741.

4. Experimental Results

The oscillator in Fig. 3 had the following circuit parameters: R=10kΩ, C=470nF, C^*=68nF, V_0=1V. Depending on control parameter R^* it generated simple sine waves, more complex 2T and 4T waves, also chaotic signals. The fundamental frequency f^* of the signals was about 33 Hz (period $T=1/f^*\approx$30ms). Several snapshots of the original $S(t)$ and the predicted signals $S(t+\tau)$ were displayed simultaneously on a screen of an oscilloscope.

4.1. First-Order Prediction

The performance of the predictor is illustrated in Fig. 4.

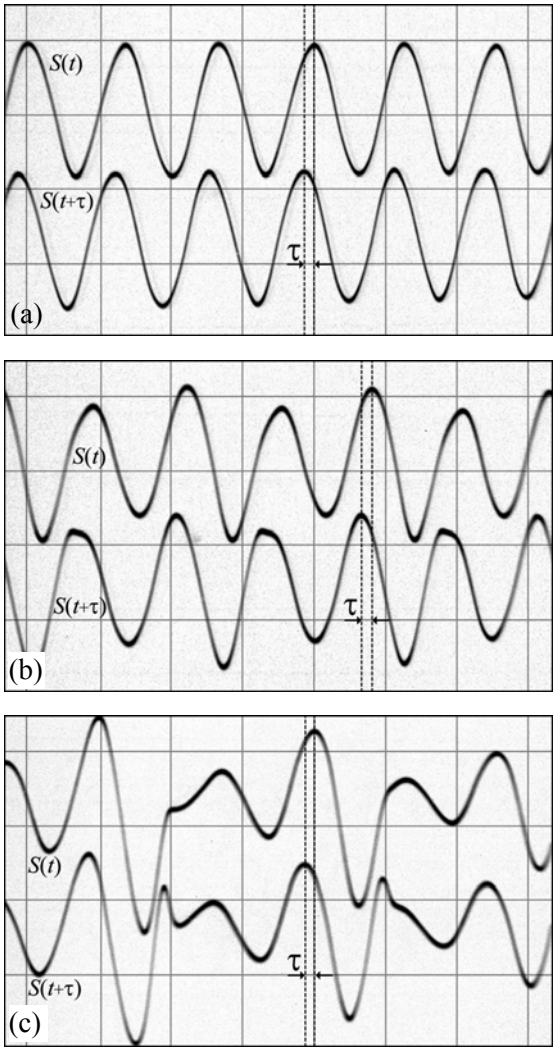

Fig. 4. Different waveforms at the input (x signals from the generator in Fig. 3) and the output of the first-order predictor (Fig. 1). For clarity the $S(t+\tau)$ trace is shifted down by 2 divisions. (a) sine-wave, (b) 2T wave, (c) chaotic signal. Vertical 1 V/div., horizontal 20 ms/div. RC=1.25ms (R=10kΩ, C=125nF), R_0=2.5kΩ, R_1=3.33kΩ. Estimated prediction $\tau=3RC$=3.75ms, ($\tau=3\varepsilon$, $|a_0|$=4, $|a_1|$=3). Measured prediction 3.0ms.

4.2. Second-Order Prediction

The performance of the second-order predictor (Fig. 2) is illustrated in Fig. 5. The results are very similar to those for the first-order predictor (Fig. 4). All the predicted signals $S(t+\tau)$ are moved to the left with respect to $S(t)$ by about 2.5 ms, i.e. by the estimated prediction time τ. There are some small distortions in the shape of the predicted signals at the time instants when the original signals $S(t)$ change abruptly. The distortions of $S(t+\tau)$ are larger in the case of 2T and chaotic signals, because of their broadband spectral content. Quantitative analysis of the distortions is presented in the next subsection 4.3.

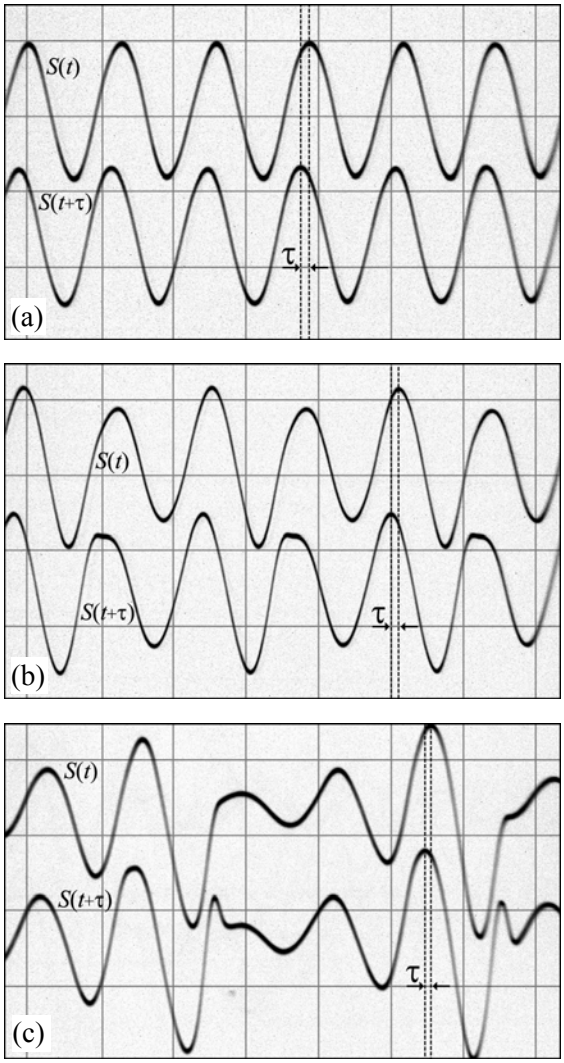

Fig. 5. Different waveforms at the input (x signals from the generator in Fig. 3) and the output of the second-order predictor (Fig. 2). For clarity the $S(t+\tau)$ trace is shifted down by 2 divisions. (a) sine-wave, (b) 2T wave, (c) chaotic signal. Vertical 1 V/div., horizontal 20 ms/div. RC=2.5ms (R=10kΩ, C=250nF), R_0=2.86kΩ, R_1=2.5kΩ, R_2=6.67kΩ. Estimated prediction $\tau=RC$=2.5ms, ($\tau=\varepsilon$, $|a_0|$=3.5, $|a_1|$=4, $|a_2|$=1.5). Measured prediction 2.6ms.

4.3. Prediction Errors

To characterize the distortions quantitatively the prediction errors have been measured in the following way. The predicted signal $S(t+\tau)$ was delayed electronically in a bucket-brigade delay line. The delay time τ_{DEL} was carefully tuned to compensate the prediction: $\tau_{DEL} = \tau$. The delayed predicted signal $S_{DEL}(t+\tau) \equiv S(t+\tau-\tau_{DEL}) = S(t+\tau-\tau)$ then was compared with the original signal. The difference between them $\Delta = S_{DEL}(t+\tau) - S(t)$ was measured by means of a differential preamplifier and a root mean square (RMS) voltmeter. The same voltmeter was used to measure the RMS value of the $S(t)$. The relative RMS error

$$RMSE = \frac{\sqrt{<\Delta^2> - <\Delta>^2}}{\sqrt{<S^2> - <S>^2}} \qquad (17)$$

was then calculated. The results for both predictors are summarized in Table 1.

Table 1. *RMSE* of the first-order predictor (RC =1.25 ms, τ_{exp} = 3.0 ms) and the second-order predictor (RC =2.5 ms, τ_{exp} = 2.6ms) for different signals.

	First-order	Second-order
Sine waves	1.4 %	1.3 %
2T waves	7.4 %	6.0 %
Chaotic waves	17 %	13 %

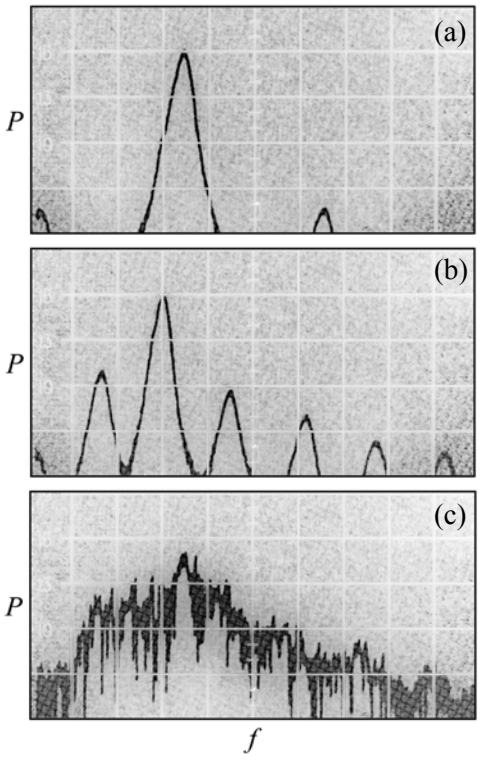

Fig. 6. Experimental power spectra $P(f)$ in the frequency range $f = 0\ldots100$ Hz. $f^* \approx 33$ Hz. (a) sine wave, (b) 2T signal, and (c) chaotic signal. Vertical scale 10 dB/div. Horizontal scale 10 Hz/div. Spectral resolution 3 Hz.

One can see from Fig. 4 and Fig. 5, also from Table 1 that there is no essential difference between the errors of the first- and the second-order predictors, while the errors grow rapidly with the complexity of the signals. The latter result can be explained by the fact that though the 2T and chaotic signals are characterized by the same fundamental frequency as the sine wave ($f^* \approx 33$ Hz), they have strong higher harmonics (Fig. 6). Therefore the RC appears to be insufficiently small. Indeed, decreasing the RC in the first-order predictor from 1.25 ms to 0.33 ms and increasing τ from $3RC$ to $11RC$ in order to restore the same prediction time of 3 ms reduces the error from 17 % to 10 % for chaotic signals. For shorter prediction, e.g. τ =1.8 ms, the error, as expected, is still lower: 5.9 %.

5. Conclusions

A simple analogue circuit containing RC active filters has been designed for prediction of time-continuous signals on a real time scale. It is suitable for any type of signals, either periodic or chaotic waves. For short prediction time experiments show relatively low distortions. Though a specific experimental prototype has been demonstrated for simplicity at low frequencies (several tenths of Hz) we believe that the frequency range can be easily extended to several tenths of MHz by replacing the LM741 with high-speed opamps, e.g. AD8001 type chips (threshold frequency f_T = 800 MHz) and reducing RC to 3 ns (R = 300 Ω, C = 10 pF). Further increase of the frequencies to several GHz for ultrafast control applications can be achieved using discrete active elements, e.g. BFG520 type transistors with f_T=9 GHz and lowering the integration parameter RC to 20 ps.

Acknowledgments

This work was partially supported by Lithuanian State Science and Study Foundation under contract No. T-33/05. We thank V. Pyragaitė for tentative numerical evaluations. On of us (A.T.) was partially supported by the EC project "The Center in Processing, Research and Application of Advanced Materials (PRAMA)" under contract No. G5MA-CT-2002-04014.

References

[1] B. C. Kuo, "Automatic control systems" (Prentice-Hall, Englewood Cliffs, NJ, 1995).

[2] J. N. Blakely, L. Illing, and D. J. Gauthier, "Controlling fast chaos in delay dynamical systems", *Phys. Rev. Lett.*, vol.92, pp.193901-1-4, 2004.

[3] P. Horowitz and W. Hill, "The art of electronics" (Cambridge University Press, New York, 1993).

[4] A. Tamaševičius, G. Mykolaitis, V. Pyragas, and K. Pyragas, "Simple chaotic oscillator for educational purposes", *Eur. J. Phys.*, vol.26, pp.61-63, 2005.